

Supplement to Hypersonic Boost-Glide Weapons

James M. Acton

This supplement contains additional sections and appendices A and B of James M. Acton, “Hypersonic Boost-Glide Weapons,” *Science & Global Security* 23 (2015), www.tandfonline.com/10.1080/08929882.2015.1087242.

Additional information can be found in a companion paper: David Wright, “Research Note to Hypersonic Boost-Glide Weapons by James M. Acton: Analysis of the Boost Phase of the HTV-2 Hypersonic Glider Tests,” *Science & Global Security* 23 (2015), www.tandfonline.com/10.1080/08929882.2015.1088734.

Tactical warning times

Some of the potential missions for boost-glide weapons would require tactical surprise for success, that is, the target state must receive insufficient warning of an incoming attack to be able to take effective countermeasures.¹ For example, the United States would only be successful in attacking North Korean ICBMs or Chinese anti-satellite weapons if the incoming gliders were not detected until it was too late for North Korea or China to launch their weapons before they were destroyed.

Warning time depends on both the characteristics of the incoming weapon and the target state’s detection capability. For illustrative purposes, two different strikes are considered here:

- a strike with a long-range weapon, very similar to the Hypersonic Technology Vehicle-2 (HTV-2), over a distance of 11,000 km (the distance from Vandenberg Air Force Base in California to central China). It is assumed that $L/D = 2.5$ and that equilibrium gliding is established, as in the planned B test flight for the HTV-2, 600 s after launch, when the vehicle is 4,200 km downrange and traveling at $6,100 \text{ ms}^{-1}$.

- a strike with a shorter-range, forward-deployed weapon, broadly similar to the Advanced Hypersonic Weapon (AHW), over a distance of 3,500 km (a plausible range for a U.S. submarine in the Pacific ocean to attack a target in central China). It is again assumed that $L/D = 2.5$ but, in this case, that equilibrium gliding is established 450s after launch, 2,500 km downrange and at a speed of $3,200 \text{ ms}^{-1}$.²

Three different types of early-warning system are considered: satellite-based infra-red sensors designed to detect missile plumes, and ballistic missile early-warning radars and modified air defense radars designed to detect incoming re-entry vehicles (RVs). Although not considered here, an area for further study is the possibility of detecting the heat signal of an incoming glider by airborne or space-based infra-red detectors.

Currently, only the United States operates satellite-based infra-red sensors (known in U.S. military jargon as overhead persistent infra-red sensors) to detect ballistic missile launches. Following a series of technical failures, none of Russia’s early-warning satellites are operational at the moment, but it had a space-based early-warning capability until 2014 (though this capability had been limited for some time) and has the stated intent to reacquire it.³ There have also been media reports that China is developing early-warning satellites too.⁴

Because a boost-glide weapon would be launched by a rocket very similar to a long-range ballistic missile—if not by a repurposed intercontinental ballistic missile (ICBM) or sea-launched ballistic missile (SLBM)—it would be detected by an appropriately positioned satellite very shortly after launch; at the latest immediately after penetrating through any clouds that happened to be present. For satellite-based early warning systems, therefore, the warning time would essentially be equal to the total weapon travel time. This time can be calculated from (S.25) and is shown in table S.1.

An alternative means to detect an incoming boost-glide weapon would be radar. The United States, Russia and China all operate large land-based radars designed to detect incoming intercontinental-range missile RVs early in flight. The differences between the boost-glide and ballistic trajectories have important implications, however, for monitoring by such radars. The HTV-2, for example, is designed to glide at an altitude of less than 50 km and to approach the target at 30–40 km. By contrast, ICBMs generally “top out” at well over 1,000 km. In consequence, an incoming hypersonic glider would be located below a radar’s horizon—that is, hidden from it by the Earth’s curvature—for much more of its trajectory than a ballistic missile. Thus radars would provide much less warning time of a boost-glide weapon attack than a ballistic missile attack.

To be precise, the distance, ℓ , at which an RV approaching a radar rises

above its horizon and into its field of view is given by

$$\ell = kr_e \left(-\theta + \sqrt{\theta^2 + 2h/kr_e} \right), \quad (\text{S.1})$$

where h is the altitude of the RV, θ is the angle of elevation of the radar (in radians), k is a dimensionless constant, and r_e is the radius of Earth. Based on a purely geometric argument, k should equal unity. However, the first-order corrections from refraction result in $k = 4/3$.⁵ If a radar is sufficiently powerful to detect an incoming RV at a distance ℓ , increasing the radar’s power further does not lengthen the detection distance. In this “horizon-limited” case, the warning time is equal to the time between the RV’s passing through the radar’s horizon and its reaching the target.

In general, ℓ increases as θ decreases. However, if θ becomes too small, the signal can get “lost” in interference from the ground. Upper and lower bounds on θ for a modern early-warning radar can be estimated from the environmental impact statement on U.S. national missile defense activities produced by the U.S. Missile Defense Agency. According to this document, the Pave Paws early-warning radar can be angled to 3° above the horizon, giving the upper bound on θ .⁶ However, the bottom of the beam extends for about one degree below its center, so a lower bound on θ is 2° . Using (S.1) with $\theta = 3^\circ$ and $h = 30$ km, a lower limit on the detection distance for a glider is about 400 km. Taking $\theta = 2^\circ$ and $h = 40$ km gives an upper limit of about 600 km. Using an intermediate value of $\ell = 500$ km and assuming that the radar is located 500 km in front of the target, warning times can be calculated using (S.25) and are shown in table S.1.

Finally, a state could attempt to use a less powerful air-defense radar to detect an incoming boost-glide weapon. In this case, the detection distance would depend on the radar cross section, σ , of the incoming RV. If a radar’s detection capability is limited by its power, rather than its horizon, then detection distance is given by

$$\ell = R_0 \sigma^{1/4}, \quad (\text{S.2})$$

where R_0 , the reference range of the radar, represents the detection distance for an object with a cross section $\sigma = 1 \text{ m}^2$. The cross section of an RV depends on both its shape and the wavelength, λ , of the incident radar waves. Since the shape of U.S. hypersonic gliders is classified an exact calculation is not possible. However, because the AHW is conical, its cross section when viewed “nose-on” is probably similar to that of a ballistic re-entry vehicle for which $\sigma \sim 0.1\lambda^2$ at relevant wavelengths.⁷ For a surveillance radar operating near 1 GHz (the lower end of the L band), the cross section of the AHW is, therefore, approximately 0.01 m^2 . The same cross section is assumed for the HTV-2, even though it is non-axisymmetric, on the grounds that, because ℓ depends only weakly on σ , even a rough approximation to the cross section can yield a reasonable approximation to detection distance.

	HTV-2 strike over 11,000 km	AHW strike over 3,500 km
Early-warning satellite	37	14
Missile early-warning radar	7	7
Air defense surveillance radar	4	4

Table S.1: **Warning time in minutes for boost-glide strikes against different early-warning systems. It is assumed that the radars are located 500 km in front of the target.**

Using (S.2) with $\sigma = 0.01 \text{ m}^2$, it follows that a sophisticated air defense radar with $R_0 = 300 \text{ km}$ would be able to detect an incoming glider at a distance of about 100 km .⁸ The resulting warning times are shown in table S.1 (again under the assumption the radar is located 500 km in front of the target.)

The values shown in table S.1 are illustrative and can change depending on the locations of the target and the radars, and the precise trajectory of the incoming weapon. What’s interesting is not so much the exact values but how different warning times can be. For example, if used against a sophisticated adversary with a satellite-based early-warning system, a long-range weapon based in the continental United States could provide militarily significant warning of an attack.⁹ This weakness reduces the value of acquiring boost-glide weapons to threaten Chinese anti-satellite capabilities or anti-ship ballistic missiles since Beijing could probably field early-warning satellites before the United States could field boost-glide weapons. The use of a shorter-range, forward-based boost-glide weapon in this scenario would reduce warning time significantly—but it would still be a marginal case that the U.S. Department of Defense should examine more closely if it is interested in acquiring the AHW or a similar system for use against China. By contrast, an adversary that has only radar technology at its disposal would be highly unlikely to gain a useful margin of tactical warning of a boost-glide strike. Thus table S.1 helps illustrate two general points about boost-glide weapons: that their military effectiveness is scenario-dependent and that different weapons have their own specific set of strengths and weaknesses.

Attacking hard and deeply buried targets

Penetration depths

A non-nuclear earth-penetrating weapon essentially consists of a high-explosive warhead protected by a metal case. In order to destroy an underground facility it must pass through the ground and into target (or at least very nearby) before the explosive is detonated. (This kill mechanism stands in contrast to the way nuclear earth-penetrators work. They do not need to

detonate close to a target but instead aim to create a large shockwave that propagates through the ground, potentially for hundreds of meters, before crushing the target.)

Based on experimental data, Sandia National Laboratories have developed a widely-used set of formulae that relates penetration depth, D_p , to the speed of a penetrator on impact, v_p . For a penetrator with $v_p > 61 \text{ ms}^{-1}$ striking a hard rock or concrete target, the relevant formula in SI units is¹⁰

$$D_p = 0.000018SN (m_p/A_p)^{0.7} (v_p - 30.5), \quad (\text{S.3})$$

where S is a dimensionless quantity representing the “penetrability” of the target, N is a dimensionless quantity that depends on the shape of the penetrator’s nose, m_p is its mass, and A_p is its cross-sectional area. This result ceases to be valid when v_p becomes so large that the penetrator deforms plastically on impact, at which point D_p starts to decrease.¹¹ There is, therefore, an optimum impact speed that maximizes penetration depth. This speed depends on the yield strength of the penetrator’s shell and is between about 1,000 and 1,200 ms^{-1} for modern materials.¹²

Existing air-dropped penetrators are reported to be able to reach speeds of between 460 ms^{-1} and 500 ms^{-1} , significantly lower than is required to maximize penetration depth.¹³ Boost-glide weapons, by contrast, could deliver a penetrator at the optimum speed. In fact, they would generally need to slow down from their cruising speeds to prevent failure of the penetrator on impact.

Given the number of unknowns in (S.3), a productive way of exploring the effectiveness of a hypothetical boost-glide penetrator is to estimate its effectiveness relative to other penetrating weapons that the United States currently possesses. This approach is not just mathematically convenient; it is also useful from a policy perspective because it focuses attention on the extent to which boost-glide weapons could augment existing U.S. capabilities. Assuming that two different penetrators (labeled 1 and 2) have similarly shaped noses, it follows from (S.3) that their relative effectiveness—that is, the ratio of their penetration depths—is given by

$$\frac{D_p^{(1)}}{D_p^{(2)}} = \left(\frac{m_p^{(1)}/A_p^{(1)}}{m_p^{(2)}/A_p^{(2)}} \right)^{0.7} \frac{v_p^{(1)} - 30.5}{v_p^{(2)} - 30.5}. \quad (\text{S.4})$$

The most effective penetrator that the United States currently possesses is the GBU-57—more commonly known as the Massive Ordnance Penetrator. It is reportedly able to penetrate to 20 m in reinforced concrete, although there is no independent confirmation of this claim.¹⁴ Data on the reported mass, length (L_p), and radius (r_p) of this weapon are shown in table S.2, along with its calculated mass-to-area ratio and average density ($\bar{\rho}_p$), assuming it is cylindrical. It has also been reported that the Massive Ordnance Penetrator contains about 2,400 kg of high explosive.

	GBU-57	GBU-28	Boost-glide penetrator
m_p (kg)	13,600	2,075	$1,250 \pm 250$
L_p (m)	6.25	5.824	5.0 ± 0.5
r_p (m)	0.4	0.185	0.16 ± 0.02
$\bar{\rho}_p$ (kg m^{-3})	4,300	3,300	$3,100 \pm 1,200$
m_p/A_p (kg m^{-2})	27,000	19,000	$15,400 \pm 5,600$
v_p (m s^{-1})	480 ± 20	480 ± 20	$1,100 \pm 100$

Table S.2: **Properties of three different earth-penetrating weapons: the GBU-57 (Massive Ordnance Penetrator), the GBU-28, and a hypothetical boost-glide delivered weapon. All quantities are defined in the text.** Sources for the data on the GBU-57 and GBU-28: “GBU-57A/B Massive Ordnance Penetrator (MOP),” *Jane’s Air-Launched Weapons* (IHS Global, February 25, 2013); “GBU-28 Paveway III and Enhanced Paveway III,” *Jane’s Air-Launched Weapons* (IHS Global, February 27, 2013).

Any estimate of the characteristics of a hypothetical boost-glide penetrator is necessarily subject to large uncertainties. David Wright’s analysis of the drop zones for the HTV-2 test flights, presented in a companion paper, suggests that the HTV-2 has a mass of around 1,000 kg. There is insufficient data to estimate the mass of the AHW.¹⁵

In any case, if boost-glide technology is successfully developed, it may be possible to fly gliders substantially heavier than the HTV-2 by trading increased weight for reduced re-entry speed (and hence reduced range). Certainly, the Minotaur IV Lite launch vehicle can carry a payload heavier than 1,000 kg. According to the environmental impact assessment for a (now-abandoned) weaponized version of the HTV-2, the Conventional Strike Missile, this booster can accommodate a payload with a maximum mass of 1,500 kg and a maximum length of 6.1 m.¹⁶ The *User’s Guide* for the Minotaur family of rockets puts the maximum payload of the Minotaur IV Lite at 3,000 kg when fired on a ballistic trajectory with a range of 6,600 km.¹⁷ Clearly, not all of the glider’s mass can go to the warhead, but it seems plausible to assume that a boost-glide penetrator might have a mass of $1,250 \pm 250$ kg, of which about 15% or 190 kg is high explosive, and might be 5 ± 0.5 m in length.

To have the same mass-to-area ratio as the GBU-57, the boost-glide penetrator would have a radius of about 0.12 m. A penetrator this thin appears to be implausible for a couple of reasons. First, this penetrator would have an average density of $5,400 \text{ kg m}^{-3}$, which is much higher than anything that has been achieved previously and appears infeasible because of the need to incorporate high explosive, which has a low density, into the structure. Second, a penetrator that is too thin would risk bending on

impact, severely reducing its effectiveness. A useful point of reference here is the GBU-28, a penetrating weapon that has a roughly similar total mass to the boost-glide penetrator and contains a similar mass of high explosive. It has a radius of 0.185 m and an average density of $3,300 \text{ kg m}^{-3}$, as shown in table S.2.

Against this background, a lower bound of $r_p = 0.14 \text{ m}$ is obtained for the boost-glide penetrator by assuming that it has the same average density as the GBU-57. It is far from clear that such a penetrator could be successfully developed. An upper bound of $r_p = 0.185 \text{ m}$ is obtained by assuming that the boost-glide penetrator has the same radius as the GBU-28. In fact, even this upper bound may be slightly optimistic as the greater speed of the boost-glide penetrator might require it to be thicker than the GBU-28. The resulting estimate of $r_p = 0.16 \pm 0.02 \text{ m}$ and the other characteristics of the hypothetical boost-glide penetrator, which can be evaluated straightforwardly from m_p , r_p and L_p , are shown in table S.2.

Using (S.4), the values shown in the table, and the usual techniques for combining uncertainties, the boost-glide penetrator is estimated to be able to penetrate more deeply than the Massive Ordnance Penetrator by a factor of 1.5 ± 0.4 . Clearly, the uncertainty is relatively large (which is inevitable given how many quantities must be estimated). Nonetheless, a boost-glide penetrator would appear to augment U.S. capabilities.

There are, however, three important caveats to this conclusion. First, the assumptions underlying it deserve further scrutiny. Second, tunneling deep into hard rock—far beyond the reach of any plausible conventional penetrator—is relatively cheap. It is unclear, therefore, how many important targets are located too deep for the Massive Ordnance Penetrator to destroy but are shallow enough for a boost-glide penetrator to reach. Third, to enable the effective use of any penetrating weapon, very accurate intelligence is needed on the target’s location and layout (unless it is so small that layout is irrelevant). Detailed information on the composition and structure of the material in which the target is buried is also required since, in some media, a penetrator’s trajectory may be curved (especially if it does not strike the ground perpendicularly).¹⁸ These challenges would be more acute with the use of a boost-glide penetrator compared to the Massive Ordnance Penetrator, given the former would contain much less high explosive and hence produce a significantly smaller blast than the latter.

Silo vulnerability

Missiles silos constitute one set of underground targets with accurately known locations. Indeed, Russian experts and officials have repeatedly expressed concern that their nuclear forces could be vulnerable to American non-nuclear weapons.¹⁹ These concerns are multi-faceted and relate to a variety of potential weapons, including shaped charges delivered by cruise

missiles.²⁰ However, Conventional Prompt Global Strike weapons have, particularly in recent months, elicited special concern.²¹

A relatively detailed description of SS-18 silos in Kazakhstan, dismantled following the fall of the Soviet Union, is available in a report published by the U.S. Defense Threat Reduction Agency in 2000. According to this report, the silo tubes in these structures were 2.95 m in radius and were protected by a door that was “on the order of one meter” thick and was made mostly of concrete inside a metal shell.²² Given that penetrating weapons can pass through much more than 1 m of reinforced concrete, it seems likely that, in the event of a direct hit on a silo door, a penetrator would pass straight through and destroy the ICBM inside (although the effect of the door’s metal shell deserves further study). If the weapon missed the silo door, however, it might still be able to destroy the ICBM inside by penetrating into the surrounding structure, exploding and creating a crater large enough to impinge upon the silo tube.

Modeling this process properly is clearly a difficult exercise, not least because a silo is a complex, inhomogeneous structure consisting of cement, metal, backfilled earth and bedrock. However, the problem can be simplified by focusing on the material immediately adjacent to the silo tube, which is either mostly cement (to a depth of 7 m) or hard rock (below that).²³ Predicting the size of a crater created by a conventional explosion in these materials is a theoretical challenge. However, some limited but relevant experimental data is available from two conventional cratering experiments, known as Buckboard and Pre-Schooner, conducted in the 1960s as part of a broader research effort into peaceful nuclear explosions.²⁴ These experiments suggest that the maximum crater size, R_c^* , and the optimum depth of burst, D_c^* , are related to the yield of the explosion, Y , by

$$R_c^* = 45Y^{1/3.4} \quad \text{and} \quad D_c^* = 50Y^{1/3.4}, \quad (\text{S.5})$$

where R_c^* and D_c^* are both measured in meters and Y is measured in kilotons of TNT.

Assuming that the boost-glide penetrator uses tritonal as its high explosive, which releases about 7% more energy per unit mass than TNT,²⁵ it would form a crater with radius $R_c^* = 4$ m if detonated at a depth $D_c^* = 4$ m (which is well within its reach). For purposes of comparison, the Massive Ordnance Penetrator would form a larger crater of radius $R_c^* = 8$ m if detonated at a depth $D_c^* = 9$ m (also well within its reach). If it is further assumed, somewhat arbitrarily, that this crater must extend 1 m into the silo tube to ensure destruction of its missile then the kill radius (the distance by which a penetrator can miss the center of the silo tube and still destroy the missile) is $r_k = 6$ m for the boost-glide penetrator and $r_k = 10$ m for the Massive Ordnance Penetrator. In turn, the kill probability, p_k , is related to r_k by

$$p_k = 1 - e^{-(r_k^2 \ln 2)/\sigma_c^2}, \quad (\text{S.6})$$

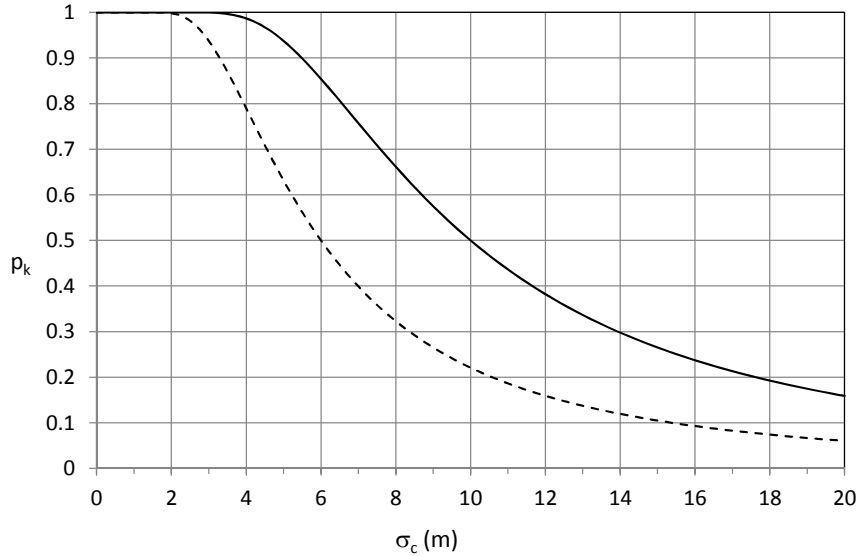


Figure S.1: **Plot of kill probability, p_k , against circular error probable, σ_c (in m), for a boost-glide penetrator (dashed line) and the Massive Ordnance Penetrator (solid line) against an SS-18 silo.**

where σ_c is the incoming weapon's circular error probable, that is, the radius of a circle in which the weapon has a 50% chance of landing. Figure S.1 shows a plot of p_k against σ_c for both the boost-glide penetrator and the Massive Ordnance Penetrator.

Clearly, these calculations are highly approximate. Nonetheless, significant uncertainties in r_k notwithstanding, two high-level conclusions can be drawn. First, it is clear from figure S.1 that, if the Massive Ordnance Penetrator and the boost-glide penetrator have similar accuracies, the former is more effective at holding silos at the risk than the latter. Second, to credibly threaten Russian silos, either weapon would need a circular error probable of a few meters.

Even if these results are confirmed by more accurate calculations, the extent to which penetrating munitions pose a credible threat to silos is still a matter for debate. While accuracies of a few meters can be obtained with GPS guidance under optimum conditions, it could be difficult in wartime when Russia would presumably try to jam U.S. GPS signals (and the United States would attempt counter-jamming efforts). It may also be possible to redesign silos so that incoming penetrators would be deflected away from the missile or perhaps even ricochet off angled structures on the surface.²⁶ Russia could also try to protect its silos with terminal defenses, raising questions highlighted above about the survivability of boost-glide weapons (which would have to slow down from their cruising speeds to deliver pene-

trating munitions) and new questions about the survivability of stealthy aircraft, including the B-2 bomber, which is the only aircraft currently capable of delivering the Massive Ordnance Penetrator. Moreover, the question of silo vulnerability does not hinge on purely technical issues; there are also political judgments to be made. For example, should Russia be concerned about a “bolt-from-the-blue” conventional first strike in peacetime? If so, Moscow would have to worry that its defenses were not on alert during a strike. Also, what does it mean to “credibly” threaten a silo? American and Russian experts might well disagree over how big a conventional weapon’s kill probability would need to be for it to create a realistic threat to a silo.

Finally, of course, a successful attack on Russia’s silo-based ICBM force would achieve very little if the United States could not also eliminate its other nuclear forces, including mobile ICBMs, SLBMs and heavy bombers. Given the relatively low alert rate of Russia’s submarines—it does not yet appear to have resumed continuous deterrent patrols in spite of a plan to do so²⁷—coupled to the apparent U.S. lead in anti-submarine warfare, Russia’s road-mobile ICBMs are probably the most survivable component of its nuclear forces.

Attacking dispersed mobile missiles

Understanding the ability of boost-glide weapons to hold mobile targets at risk is important in a number of contexts. First, both Russia and China are concerned, in spite of American protestations to the contrary, that these weapons could target their nuclear-armed, mobile ballistic missiles.²⁸ Second, the possibility of acquiring CPGS weapons to threaten two types of *non*-nuclear Chinese capabilities—its anti-satellite weapons and its anti-access/area-denial systems—has been raised by high-level officials and in important government documents.²⁹ China’s anti-satellite capabilities include direct-ascent weapons carried on mobile launchers.³⁰ Its anti-access/area-denial capabilities are designed to hinder U.S. forces from entering the west Pacific in a conflict and to curtail their freedom of movement within the theater. These weapons include non-nuclear, mobile ballistic missiles, such as the land-attack DF-21C and the anti-ship DF-21D. Finally, the United States has stated explicitly that CPGS weapons could be acquired to target nuclear-armed ballistic missiles in North Korea and, perhaps in the future, Iran.³¹

In general, there are two approaches to attacking a mobile missile: wait until it is stationary or attack while it is on the move. The latter is certainly preferable but places greater demands on intelligence, surveillance and reconnaissance and requires that the incoming weapon be able to accept in-flight target updates. In either case, there is likely to be some uncertainty in the location of the target—although this uncertainty is almost certain to

be greater in the case of a moving missile. This uncertainty is characterized by the target location error, σ_t , which can be defined, analogously to the circular error probable, as the radius of the circle in which the target has a 50% chance of being located. The magnitude of σ_t depends upon both the characteristics of the target’s motion and the effectiveness of the attacker’s intelligence, surveillance and reconnaissance system. However, assuming that the errors in both the location of the target and the impact point of the incoming weapon are uncorrelated Gaussian random variables, then the requirement for the incoming weapon to be effective is

$$r_k \gg \sqrt{\sigma_c^2 + \sigma_t^2}, \quad (\text{S.7})$$

where, as before, σ_c is its circular error probable and r_k is its kill radius. The remainder of this section is devoted to estimating r_k for a boost-glide weapon.

Plans to weaponize the HTV-2 called for it to be armed with a particle dispersion warhead with a total mass of about 390 kg consisting of 70 kg to 90 kg of high explosive and “several thousand debris particles, each measuring no more than a few centimeters...in diameter.”³² The high explosive in this kind of weapon is detonated shortly before impact in order to create an expanding cloud of debris particles. These particles aim to damage the target through their kinetic energy (the high explosive plays no direct role in effecting this damage). Changing the height at which the explosive is detonated changes the size of the weapon’s “footprint” on the ground. Clearly, a large footprint is desirable to mitigate uncertainty about the location of a mobile target. However, increasing the size of the footprint reduces the density of debris particles, increasing the probability that, even if the weapon’s footprint overlaps the target, none of them hit it.³³ There is, therefore, a trade-off involved in choosing the size of the footprint.

For a particle dispersion warhead mounted on a boost-glide weapon, the kinetic energy of the debris particles could be extremely large. For example, if there were 4,000 particles in the warhead with a combined mass of 300 kg, and if the weapon reached the target at “only” $2,000 \text{ ms}^{-1}$, then the kinetic energy of each particle would be $150,000 \text{ J}$.³⁴ By way of comparison, a particle with an energy of $20,000 \text{ J}$ is required to inflict heavy damage on an aircraft.³⁵ An energy of $150,000 \text{ J}$ therefore seems more than sufficient to penetrate the missile skin and any protective canister, providing it is not too highly armored (which seems unlikely given the weight constraints imposed by mobility).

It is assumed here that a ballistic missile can be effectively disabled by penetrating its motor with even a single debris particle. There are various possible failure modes. For example, solid-rocket motors can malfunction if there are cracks or voids in the fuel—precisely the kind of damage that a debris particle could inflict. Alternatively, the escape of gases through

the hole in the casing could cause the missile to tumble out of control, as occurred during some Minuteman I and II flight tests after a malfunction caused accidental venting through a cover in the missile casing.³⁶

That said, it is straightforward to generalize the method presented below to account for a greater damage requirement than a direct hit from at least one particle. Indeed, it is possible that U.S. requirements might be more stringent, especially if the target missiles were nuclear-armed. For example, during the Cold War, U.S. nuclear war plans called for Soviet mobile missiles to be physically flipped over (although this requirement may have had more to do with facilitating battle damage assessment than destroying the target *per se*).³⁷

The target missile's motor is modeled here as a cylinder of length a and diameter b . It is assumed that the particle dispersion weapon, which contains N_p debris particles, produces a circular footprint on the ground of radius r_w . The probability that the missile is hit by at least one debris particle is denoted by $\Pi(r_w, d_m)$, where d_m is the miss distance, that is, the distance between the center of the missile and the center of the weapon's footprint. As shown in figure S.2, the area of overlap between this footprint and the missile is denoted by $A_o(r_w, d_m, \alpha)$, where α is the angle between the long axis of the missile and the line joining the center of the missile to the center of the weapon footprint.

If the area of the footprint is much bigger than the area of the missile and if the particles are homogeneously distributed within the footprint then the number of particles hitting the missile is a Poisson-distributed random variable. The mean of this distribution, $\lambda(r_w, d_m)$, is given by

$$\lambda(r_w, d_m) = N_p \frac{\langle A_o(r_w, d_m, \alpha) \rangle_\alpha}{\pi r_w^2}, \quad (\text{S.8})$$

where $\langle \dots \rangle_\alpha$ denotes an average over α . Assuming that the weapon is equally likely to miss the missile in every direction, $\langle A_o(r_w, d_m, \alpha) \rangle_\alpha$ is given by

$$\langle A_o(r_w, d_m, \alpha) \rangle_\alpha = \frac{1}{2\pi} \int_0^{2\pi} d\alpha A_o(r_w, d_m, \alpha). \quad (\text{S.9})$$

Given the number of particles hitting the missile can be modeled by a Poisson distribution, the probability that all of them miss is $\exp[-\lambda(r_w, d_m)]$, from which it follows that

$$\Pi(r_w, d_m) = 1 - e^{-\lambda(r_w, d_m)}. \quad (\text{S.10})$$

In general, $\Pi(r_w, d_m)$ must be evaluated numerically. However, it can be evaluated algebraically in two limits. First, if the miss distance is small enough that $d_m \leq d_m^-$ where

$$d_m^- = r_w - \sqrt{\frac{a^2}{4} + \frac{b^2}{4}}, \quad (\text{S.11})$$

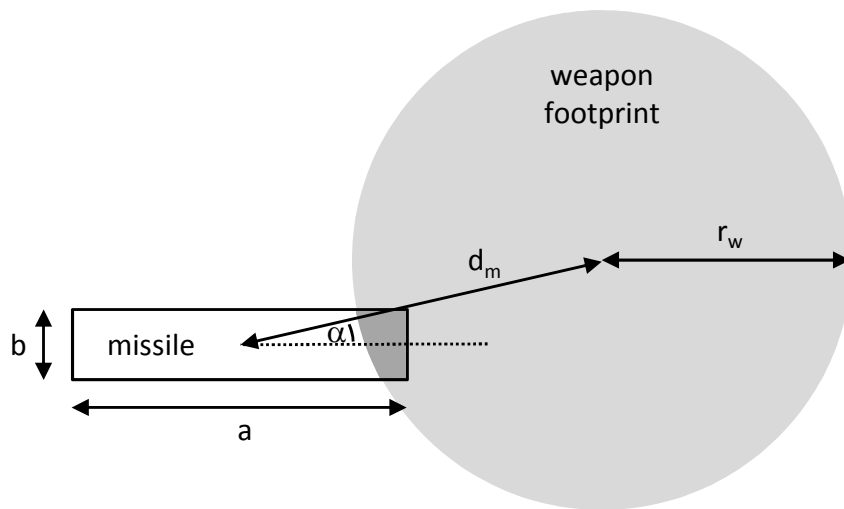


Figure S.2: Schematic diagram of the use of a particle dispersion weapon to attack a mobile missile. The area highlighted in dark gray is the area of overlap between the weapon footprint and the missile, $A_o(r_w, d_m, \alpha)$. Other quantities are defined in the main text.

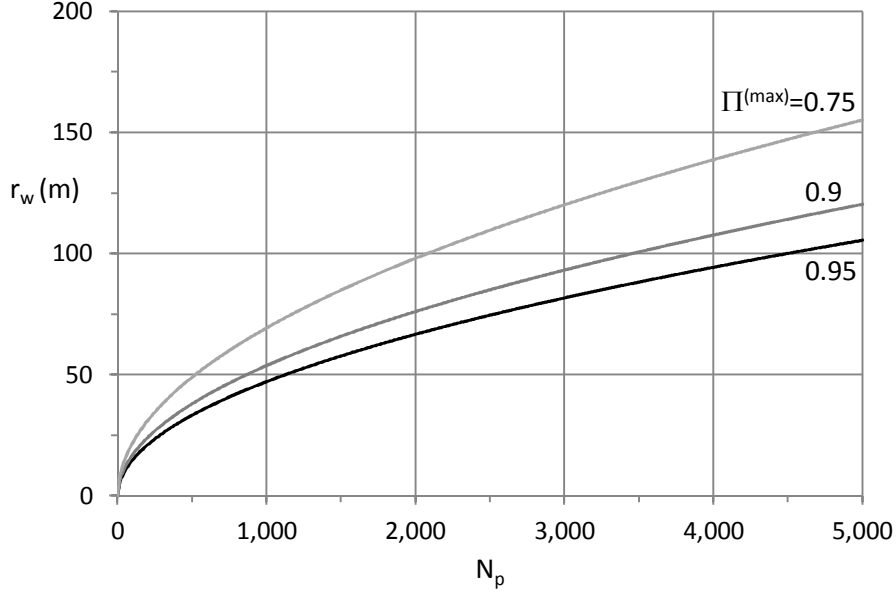


Figure S.3: **Plot of the radius of a particle dispersion weapon's footprint, r_w (in m), needed to achieve a kill probability of $\Pi^{(\max)}$ at small miss distances, against the number of particles in the weapon, N_p .**

then the missile is entirely contained within the incoming weapon's footprint for all α and $\langle A_o(r_w, d_m, \alpha) \rangle_\alpha = ab$. In this case, $\Pi(r_w, d_m)$ takes its maximum value, denoted as $\Pi^{(\max)}$, which is given by

$$\Pi^{(\max)} = 1 - \exp\left(-\frac{N_p ab}{\pi r_w^2}\right). \quad (\text{S.12})$$

This result can be used to choose r_w to ensure that the density of particles in the debris cloud is large enough that, when the incoming weapon misses the target missile by only a small distance, the kill probability reaches its desired value.

As d_m increases beyond d_m^- , the target missile is not contained within the weapon footprint for all α (which is the scenario shown in figure S.2), and $\langle A_o(r_w, d_m, \alpha) \rangle_\alpha$ and $\Pi(r_w, d_m)$ both decrease. They vanish if the incoming weapon misses the missile by a distance $d_m \geq d_m^+$ where

$$d_m^+ = r_w + \sqrt{\frac{a^2}{4} + \frac{b^2}{4}}, \quad (\text{S.13})$$

so that its footprint does not overlap with the missile for any α .

As an example, consider attempting to destroy a mobile missile with a cylindrical motor for which $a = 14$ m and $b = 1.5$ m. Figure S.3 shows, for

three particular values of $\Pi^{(\max)}$, how the required value of r_w varies with N_p . For example, if the particle dispersion weapon contains 4,000 particles, and a value of $\Pi^{(\max)} = 0.95$ is required (which seems appropriate if the target missile is nuclear armed), then the weapon footprint should have a radius of 94 m.

For these values, $N_p = 4,000$ and $r_w = 94$ m, figure S.4 shows how the kill probability varies with the miss distance, calculated numerically from (S.10) using *Mathematica*. When the miss distance is smaller than $d_m^- = 87$ m, the kill probability assumes its maximum value, $\Pi^{(\max)} = 0.95$. It then decreases, in a relatively thin band, vanishing when the miss distance is greater than $d_m^+ = 102$ m. The lethal radius of this weapon—defined as the miss distance at which the kill probability drops to, say, 0.9—can be seen from the graph to be 92 m, i.e. slightly less than r_w .

By way of comparison, if the boost-glide weapon were fitted with an explosive warhead containing 300 kg of a very energetic explosive (equivalent to, say, 500 kg of TNT), it would produce an overpressure of only 1 psi ($6,900 \text{ N m}^{-2}$) or so at a distance of 90 m.³⁸ An overpressure of this magnitude would probably not be sufficient to disable a mobile missile.³⁹ It therefore appears that boost-glide weapons would be more effective at attacking mobile missiles if armed with a particle dispersion warhead rather than an explosive warhead, which may explain why the Pentagon planned to arm the Conventional Strike Missile with the former. Whether either type of weapon would be effective in absolute terms depends, however, on both σ_c and σ_t .

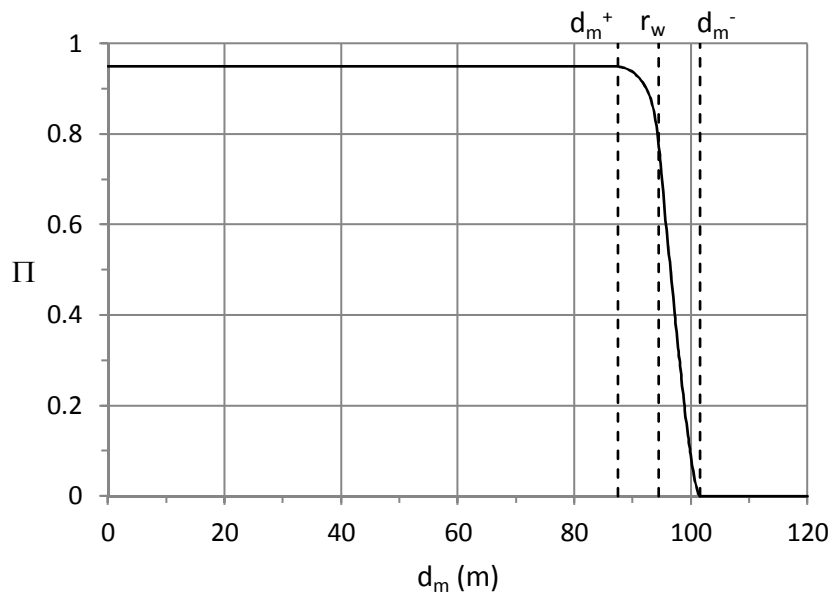


Figure S.4: Plot of the kill probability of a particle dispersion weapon, Π , against its miss distance, d_m (in m). The incoming weapon contains $N_p = 4,000$ debris particles and its footprint has a radius of $r_w = 94$ m. The target missile has a length of $a = 14$ m and a diameter of $b = 1.5$ m. Other quantities are defined in the main text.

Appendices

The quantities used in these appendices are defined in the main article (see the reference in boxed text at the start of this supplement.)

A Summary of standard derivations

Direct re-entry

The standard solution for the direct entry of a non-lifting RV is useful for analyzing a boost-glide trajectory if, during the early stages of endo-atmospheric flight, the glider is oriented to generate minimal lift in order to avoid skipping off the atmosphere.⁴⁰ Numerical simulations of this scenario indicate that for $\theta_2 > 5^\circ$, it is a good approximation to treat the path angle as a constant, that is, $\theta = \theta_2$. From this assumption it immediately follows that the relationship between downrange distance and altitude is given by

$$h_2 - h = (x - x_2) \tan \theta_2. \quad (\text{S.14})$$

If is further assumed that the drag force acting on the RV is much greater than gravity then (3) reduces to

$$\frac{dv}{dt} = -\frac{\rho_0}{2\beta_S} v^2 e^{-h/H}. \quad (\text{S.15})$$

Combining this equation with (6) yields the standard result for the variation of v with h :

$$v = v_2 e^\delta \exp\left(-\frac{H\rho_0}{2\beta_S \sin\theta_2} e^{-h/H}\right), \quad (\text{S.16})$$

where δ is a constant given by

$$\delta = \frac{H\rho_0}{2\beta_S \sin\theta_2} e^{-h_2/H}. \quad (\text{S.17})$$

The relationship between altitude and time can be found by combining (6) and (S.16) to yield a separable first-order differential equation with the solution:

$$t - t_2 = -\frac{1}{v_2 e^\delta \sin\theta_2} \int_{h_2}^h dh \exp\left(\frac{H\rho_0}{2\beta_S \sin\theta_2} e^{-h/H}\right). \quad (\text{S.18})$$

Although this integral does not have a closed form, it can be conveniently expressed in the form of a power series:

$$t - t_2 = \frac{h_2 - h}{v_2 e^\delta \sin\theta_2} + \frac{H}{v_2 e^\delta \sin\theta_2} \sum_{n=1}^{\infty} \frac{\delta^n}{n \cdot n!} \left(e^{-n(h-h_2)H} - 1 \right). \quad (\text{S.19})$$

It should be noted that if atmospheric drag can be neglected entirely (i.e. when $\beta_s \rightarrow \infty$ or $\rho_0 = 0$) then $t - t_2 = (h_2 - h)/v_2 \sin\theta_2$, which is simply the time taken for an object traveling at speed v_2 and path angle θ_2 to drop a distance $h_2 - h$ in the absence of gravity.

Equilibrium gliding

Once equilibrium gliding has been established, the glider's path angle remains close to zero and changes only slowly. This limit was first discussed in the 1930s and has been explored extensively.⁴¹ Under the assumptions that $\theta \ll 1$ rad, $d\theta/dt \approx 0$, and $g \sin\theta \ll dv/dt$, the equations of motion reduce into⁴²

$$\frac{dv}{dt} = -\frac{\rho}{2\beta_L}v^2 \quad (\text{S.20})$$

and

$$g - \frac{v^2}{r_e} - \frac{\rho}{2\beta_L} \frac{L}{D} v^2 = 0. \quad (\text{S.21})$$

Physically, the second of these equations represents a scenario in which the weight of the glider is balanced by the combination of lift and centrifugal “force.” Equilibrium is possible at only one altitude, which is given by

$$h = H \ln \left(\frac{\rho_0 r_e L}{2\beta_L D} \frac{v^2}{v_e^2 - v^2} \right). \quad (\text{S.22})$$

Combining (S.20) and (S.21) yields the differential equation

$$\frac{dv}{dt} = -g \frac{D}{L} \left(1 - \frac{v^2}{v_e^2} \right), \quad (\text{S.23})$$

which has the solution

$$\frac{v}{v_e} = \frac{\exp \left[-2 \frac{D}{L} \frac{g}{v_e} (t - t_4) \right] - \Gamma_4}{\exp \left[-2 \frac{D}{L} \frac{g}{v_e} (t - t_4) \right] + \Gamma_4}, \quad (\text{S.24})$$

where $\Gamma_4 = (1 - v_4/v_e)/(1 + v_4/v_e)$ is a function of the speed of the RV at the start of the glide phase. Given that when θ is small, $v = dx/dt$, it follows that the downrange distance of the glider as a function of time is given by

$$x - x_4 = -v_e (t - t_4) + r_e \frac{L}{D} \ln \left(\frac{1 + \Gamma_4}{\exp \left[-2 \frac{D}{L} \frac{g}{v_e} (t - t_4) \right] + \Gamma_4} \right). \quad (\text{S.25})$$

The path angle can be found from (6), noting that $dh/dt = (dh/dv)(dv/dt)$, where dv/dt is given by (S.20) and dh/dv can be found from (S.22):

$$\sin \theta = 2 \left[\frac{r_e L}{H D} \left(\frac{v}{v_e} \right)^2 \right]^{-1}. \quad (\text{S.26})$$

Because $r_e \gg H$, the assumption that $\theta \ll 1$ is self-consistent except at low speeds.

From (S.24), the time at which the glider's speed vanishes, t_5^{\max} , is given by

$$t_5^{\max} = \frac{v_e}{2g} \frac{L}{D} \ln \left(\frac{1}{\Gamma_4} \right). \quad (\text{S.27})$$

Inserting t_5^{\max} into (S.25) yields the expression for the glide range given in (1). This result must be treated with a degree of caution since, at low speeds, θ becomes significantly different from zero and thus the approximations underlying this model break down. Moreover, the assumption that L/D is constant is also likely to become increasingly invalid at low speeds. Indeed, the unphysical behavior of this model at low speeds is most obviously illustrated by the fact that it predicts that, after t_5^{\max} , the glider actually reverses direction. Nonetheless, since the glider traverses the vast majority of its course at hypersonic speeds, (1) should be a reasonable approximation for the true glide range. In general, however, it is an over-estimate.

Cross-range maneuvering

A glider can maneuver in a transverse direction by banking at an angle ψ (see figure 5). Under the same assumptions used in the previous subsection, and further assuming that the Earth's curvature in the Y-direction can be neglected, it is straightforward to calculate $\omega(t)$, the angle between the glider's velocity and the X-axis. More complex derivations, under less restrictive assumptions, are presented elsewhere.⁴³

If $v_X(t)$ and $v_Y(t)$ are the components of the glider's velocity in the X and Y directions at time t then $\tan \omega(t) = v_Y(t)/v_X(t)$. A short time, dt , later, ω changes to $\omega + d\omega$ where

$$\tan(\omega + d\omega) = \frac{v_Y + (dv_Y/dt) dt}{v_X + (dv_X/dt) dt}. \quad (\text{S.28})$$

From this expression it follows that

$$\frac{d\omega}{dt} = \cos \omega \sin \omega \left(\frac{1}{v_Y} \frac{dv_Y}{dt} - \frac{1}{v_X} \frac{dv_X}{dt} \right). \quad (\text{S.29})$$

Using Newton's Second Law, the acceleration of the glider in the X- and Y-directions is given by

$$m \frac{dv_X}{dt} = -D \cos \omega - L \sin \psi \sin \omega \quad (\text{S.30})$$

$$m \frac{dv_Y}{dt} = L \sin \psi \cos \omega - D \sin \omega. \quad (\text{S.31})$$

Substituting these two expressions into (S.29) gives

$$\frac{d\omega}{dt} = \frac{D}{mv} \frac{L}{D} \sin \psi. \quad (\text{S.32})$$

Finally, writing $d\omega/dt = (d\omega/dv)(dv/dt)$, using (S.20) and $D = m\rho v^2/2\beta_L$ gives

$$\frac{d\omega}{dv} = -\frac{1}{v} \frac{L}{D} \sin\psi, \quad (\text{S.33})$$

which can be integrated to yield (26).

B Fitting the model to HTV-2 flight test data

Table S.3 lists the known quantities about the A flight and the unknowns that are to be determined. Using the model set out in table 1, it is possible to write down 12 equations relating these 12 unknowns. For example, using (20), the five unknowns, L/D , R , v_3 , θ_4 , and v_4 are related by

$$\theta_2 - \theta_4 = \frac{L}{D} \left(1 + \frac{R}{r_e} - \frac{gR}{v_3^2} \right) \frac{v_3 - v_4}{v_3}. \quad (\text{S.34})$$

Similarly, it follows from (16) that L/D , R , v_3 , h_i and t_3 are related by

$$M_i v_s(h_i) = v_3 \left(1 - \frac{D}{L} \frac{v_3(t_i - t_3)}{R} \right). \quad (\text{S.35})$$

If h is measured in m then $v_s(h)$, measured in ms^{-1} , can be approximated by⁴⁴

$$v_s(h) = \begin{cases} 0.00175h + 247.1 & \text{if } 32,000 \leq h < 47,240 \\ 329.8 & \text{if } 47,240 \leq h < 51,110 \\ -0.00172h + 417.7 & \text{if } 51,110 \leq h < 71,000. \end{cases} \quad (\text{S.36})$$

The resulting set of equations can be solved numerically. For this work, the FindRoot routine in *Mathematica* was used.

knowns	$t_2, h_2, v_2, \theta_2, t_i, M_i, t_4, t_5, h_5, x_5 - x_2$
unknowns	$L/D, R, \beta_L, \beta_S, t_3, h_3, v_3, h_i, h_4, v_4, \theta_4, v_5$

Table S.3: **Known and unknown quantities for the A flight. The values of the known quantities are shown in table 2.**

Endnotes

¹James M. Acton, *Silver Bullet? Asking the Right Questions About Conventional Prompt Global Strike* (Washington, DC: Carnegie Endowment for International Peace, 2013), 67-71, <http://carnegieendowment.org/files/cpgs.pdf>.

²These figures are essentially notional but imply that, after traveling a distance of 3,800 km—the distance flown in the AHW test flight—the glider would be traveling at about $1,000 \text{ ms}^{-1}$ and that its average speed over the whole of the glide would be about $2,200 \text{ ms}^{-1}$. This latter figure is broadly consistent with an unconfirmed media report that the AHW flew at Mach 8. See Noah Shachtman, “2,400 Miles in Minutes? No Sweat! Hypersonic Weapon Passes ‘Easy’ Test,” *Danger Room* (blog), *Wired*, November 17, 2011, <http://www.wired.com/dangerroom/2011/11/2400-miles-in-minutes-hypersonic-weapon-passes-easy-test/>.

³Pavel Podvig, “Russia Lost All its Early-Warning Satellites,” *Russian Strategic Nuclear Forces* (blog), February 11, 2015, http://russianforces.org/blog/2015/02/russia_lost_all_its_early-warn.shtml.

⁴“China Seen Ready to Space-Based Warning Sensor,” Global Security Newswire, July 25, 2013, <http://www.nti.org/gsn/article/china-seen-readying-space-based-warning-sensor/>. For useful discussions of the underlying technology see Geoffrey Forden, *A Constellation of Satellites for Shared Missile Launch Surveillance* (Program on Science, Technology, and Society, Massachusetts Institute of Technology, July 9, 2006), <http://web.mit.edu/stgs/pdfs/white%20paper--%20A%20Multinational%20Missile%20Launch%20Surveillance%20Network.pdf>; Zia Mian, R. Rajaraman, and M. V. Ramana, “Early Warning in South Asia—Constraints and Implications,” *Science & Global Security* 11, nos. 2–3 (2003): 124–26, <http://www.princeton.edu/sgs/publications/sgs/pdf/11%202-3%20Mian%20p109-150.pdf>. Both Russia and the United States have commenced modernization of their space-based early-warning systems since these articles were written.

⁵See, for example, David J. Murrow, “Height Finding and 3D Radar” in *Radar Handbook*, 2nd ed., ed. Merrill I. Skolnik, 20.17 (Boston: McGraw Hill, 1990).

⁶Missile Defense Agency, *National Missile Defense Deployment: Final Environmental Impact Statement*, July 1, 2000, vol. 4, appendix H, 1-6, http://www.mda.mil/global/documents/pdf/env_gmd_eis_append_h.pdf.

⁷Mian, Rajaraman, and Ramana, “Early Warning in South Asia,” 149. In fact, when the wavelength of the incident radiation is similar to the size of the RV, σ oscillates between $0.5\lambda^2$ and $0.05\lambda^2$.

⁸See, for example, the Russian 96L6 surveillance radar, which is used in the S-300 air defense system. Duncan Lennox, *Jane’s Strategic Weapon Systems*, 55th issue (Coulsdon: IHS Global, July 2011), 320. See also Committee on Review and Evaluation of the Air Force Hypersonic Technology Program, Air Force Science and Technology Board, and Commission on Engineering and Technical Systems, National Research Council, *Review and Evaluation of the Air Force Hypersonic Technology Program* (Washington, DC: National Academy Press, 1998), 54, http://www.nap.edu/catalog.php?record_id=6195.

⁹For a more detailed discussion of what might constitute military significance see Acton, *Silver Bullet?*, 67.

¹⁰C. W. Young, *Penetration Equations*, SAND97-2426 (Albuquerque, NM: Sandia National Laboratories, October 1997), A-2, http://www.globalsecurity.org/military/library/report/1997/penetration_equations.pdf.

¹¹For a more detailed discussion see Robert W. Nelson, “Low-Yield Earth-Penetrating Nuclear Weapons,” *Science & Global Security* 10, no. 1 (2002): 5, <http://scienceandglobalsecurity.org/archive/sgs10nelson.pdf>.

¹²See, for example, Nancy F. Swinford and Dean A. Kudlick, *A Hard and Deeply Buried Target Defeat Concept* (Sunnyvale, CA: Lockheed Martin Missiles & Space, 1996), 1, <http://www.dtic.mil/cgi-bin/GetTRDoc?AD=ADA318768>; Defense Science Board, *Time Critical Conventional Strike From Strategic Standoff* (Washington, DC: Office of the Under Secretary of Defense for Acquisition, Technology, and Logistics, March 2009), 26, <http://www.acq.osd.mil/dsb/reports/ADA498403.pdf>.

¹³Swinford and Kudlick, *A Hard and Deeply Buried Target Defeat Concept*, 1.

¹⁴“GBU-57A/B Massive Ordnance Penetrator (MOP),” *Jane’s Air-Launched Weapons* (IHS Global, February 25, 2013).

¹⁵For its first test flight, the AHW was boosted by a modified Polaris A3 SLBM, which is less powerful than the Minotaur IV Lite rocket, which is a modified MX/Peacekeeper ICBM and was used in the HTV-2 test flights. U.S. Army Space and Missile Defense Command/Army Forces Strategic Command, *Advanced Hypersonic Weapon Program: Environmental Assessment*, June 2011, 2-2, <http://www.smdcen.us/pubdocs/files/AHW%20Program%20FEA--30Jun11.pdf>. If all other things were equal, this would suggest that the AHW is less massive than the HTV-2. However, because the AHW appears to begin its glide at a lower speed than the HTV-2, this inference is not necessarily correct.

¹⁶Acquisition Civil/Environmental Engineering, Space and Missile Systems Center, *Environmental Assessment for Conventional Strike Missile Demonstration*, August 2010, 9, <http://www.dtic.mil/dtic/tr/fulltext/u2/a544112.pdf>.

¹⁷*Minotaur IV, V, VI: User’s Guide*, release 2.0 (Chandler, AZ: Orbital Sciences Corporation, June 2013), 2.

¹⁸P. S. Bulson, *Explosive Loading of Engineering Structures* (London: E & FP Spon, 1997), 147–9.

¹⁹For a discussion of these concerns see Acton, *Silver Bullet?*, 120–25.

²⁰Yevgeny Miasnikov, “Precision-Guided Conventional Weapons” in *Nuclear Reset: Arms Reduction and Nonproliferation*, eds. Alexei Arbatov and Vladimir Dvorkin, trans. ed. Natalia Bubnova, 444 (Moscow: Carnegie Moscow Center, 2012), http://carnegieendowment.org/files/nuclear_reset_Book2012_web.pdf.

²¹Vladimir Putin, Presidential Address to the Federal Assembly, Moscow, December 12, 2013 (official translation available from <http://eng.kremlin.ru/transcripts/6402>).

²²John R. Matzko, *Inside a Soviet ICBM Silo Complex: The SS-18 Silo Dismantlement Program at Derzhavinsk, Kazakhstan*, DTRA-TR-99-15 (Dulles, VA: Defense Threat Reduction Agency, August 2000), 7–8, <http://www.dtic.mil/cgi-bin/GetTRDoc?AD=ADA388848>.

²³*Ibid.*, 7–8 and 27.

²⁴J. Toman, “Results of Cratering Experiments,” IAEA-PL-388/16 in *Peaceful Nuclear Explosions: Phenomenology and Status Report 1970* (Vienna: International Atomic Energy Agency, 1970), 368. It is unclear from this paper over what range of yields (S.5) is valid. The data points included in the graph on p. 368 were from 20 t conventional explosions. However, the Buckboard experiments used explosions as low as 0.5 t. This uncertainty underlines the approximate nature of the calculations presented here.

²⁵Michael M. Swisdak, Jr. and Jerry M. Ward, “The New DDESB Blast Effects Computer,” 28th DoD Explosives Safety Seminar, August 1998, 8, <http://handle.dtic.mil/100.2/ADA513568>.

²⁶I am grateful to David Wright for this suggestion.

²⁷Hans M. Kristensen and Robert S. Norris, “Russian Nuclear Forces, 2014,” *Bulletin of the Atomic Scientists* 70, no. 2 (2014): 80, <http://bos.sagepub.com/content/70/2/75.full.pdf>.

²⁸The United States pledged, in its 2010 Nuclear Posture Review, that CPGS weapons would “not negatively [affect] the stability of our nuclear relationships with Russia or China.” U.S. Department of Defense, *Nuclear Posture Review Report*, April 2010, 34, <http://archive.defense.gov/npr/docs/2010%20Nuclear%20Posture%20Review%20Report.pdf>.

²⁹For examples see Acton, *Silver Bullet?*, 17–21.

³⁰Jim Wolf, “China Poses Risk to Key U.S. Satellites: Top General,” Reuters, April 11, 2007, <http://www.reuters.com/article/2007/04/11/us-space-usa-china-idUSN1125395120070411>.

³¹White House, *Report on Conventional Prompt Global Strike in Response to Condition 6 of the Resolution of Advice and Consent to Ratification of the New START Treaty*, February 2, 2011, 7. For other examples see Acton, *Silver Bullet?*, 14–6.

³²Acquisition Civil/Environmental Engineering, Space and Missile Systems Center, *Environmental Assessment for Conventional Strike Missile Demonstration*, 9.

³³For this reason, the kill probability is not simply given by (S.6) with σ_c^2 replaced by $\sigma_c^2 + \sigma_t^2$.

³⁴The mass of each particle would be 0.075 kg. If the particles were spherical and made from steel with a density of $8,000 \text{ kg m}^{-3}$, each would have a radius of 2.6 cm, which is consistent with the description of the proposed Conventional Strike Missile warhead.

³⁵Craig M. Payne, ed., *Principles of Naval Weapons Systems*, 2nd ed. (Annapolis, MD: Naval Institute Press, 2010), 352.

³⁶Air Force Center for Studies and Analyses, Directorate for Strategic Force Analyses, Missile Division, *Effectiveness of the Minuteman II Stage III Refurbishment Program* (Department of the Air Force: January 1985), 3, <http://www.dtic.mil/dtic/tr/fulltext/u2/a363899.pdf>.

³⁷Matthew G. McKinzie, Thomas B. Cochran, Robert S. Norris, and William M. Arkin, *The U.S. Nuclear War Plan: A Time for Change* (Natural Resources Defense Council, June 2001), 54, available from <http://www.nrdc.org/nuclear/warplan/index.asp>.

³⁸See, for example, Payne, ed., *Principles of Naval Weapons Systems*, 349 for the methodology for calculating the overpressure produced in a conventional explosion.

³⁹An overpressure of 1 psi is only sufficient to cause light damage to unprotected troops and so appears inadequate to disable a mobile missile. Payne, ed., *Principles of Naval Weapons Systems*, 350. Reliable information on what overpressure would be needed to destroy a mobile missile is hard to come by and presumably depends significantly on the design on the missile. A 1981 study by the Office of Technology Assessment into basing modes for the MX ICBM discussed missiles designed to withstand overpressures of at least 4 psi. Office of Technology Assessment, U.S. Congress, *MX Missile Basing* (Washington, DC: 1981), 258-60, <http://ota.fas.org/reports/8116.pdf>. Of course, a mobile MX missile (which was not ultimately the variant chosen for deployment) might have been able to withstand greater overpressures than Iranian or North Korean mobile missiles, or even Chinese ones. A plausible lower limit for the overpressure that one of these missiles could withstand is perhaps 3 psi—the approximate overpressure needed to cause severe damage to a parked aircraft (which seems like a reasonable surrogate for a mobile missile). Payne, ed., *Principles of Naval Weapons Systems*, 350.

⁴⁰See, for example, Carl Gazley, Jr., “Atmospheric Entry” in *Handbook of Astronautical Engineering*, ed. Heinz Hermann Koelle (New York: McGraw-Hill Book Company, 1961), 10-10–10-13.

⁴¹Alfred J. Eggers, Jr., H. Julian Allen, and Stanford E. Neice, *A Comparative Analysis of the Performance of Long-Range Hypervelocity Vehicles*, Report 1382 (Washington, DC: National Advisory Committee for Aeronautics, [1958]), http://ntrs.nasa.gov/archive/nasa/casi.ntrs.nasa.gov/19930092363_1993092363.pdf.

⁴²Gazley, “Atmospheric Entry,” 10-14–10-16.

⁴³S. Y. Chen, *The Longitudinal and Lateral Range of Hypersonic Glide Vehicles with Constant Bank Angle*, Memorandum RM-4630-PR (Santa Monica, CA: RAND Corporation, January 1966), <http://www.dtic.mil/cgi-bin/GetTRDoc?Location=U2&doc=GetTRDoc.pdf&AD=AD0629124>.

⁴⁴Regression using data from National Oceanic and Atmospheric Administration, National Aeronautics and Space Administration, and United States Air Force, *U.S. Standard Atmosphere, 1976*, NOAA-S/T 76-1562 (Washington, DC: U.S. Government Printing Office, October 1976), <http://www.dtic.mil/cgi-bin/GetTRDoc?Location=U2&doc=GetTRDoc.pdf&AD=ADA035728>.